

# Coexistence of fusion hindrance and enhancement in the systems $^{18}\text{O} + ^{58,60,64}\text{Ni}$ <sup>a</sup>

D. Pereira<sup>1</sup>, C. P. Silva<sup>1</sup>, J. Lubian<sup>2</sup>, E. S. Rossi Jr<sup>1</sup>, L. C. Chamon<sup>1</sup>, G. P. A. Nobre<sup>1</sup> and J. J. S. Alves<sup>2</sup>

<sup>1</sup> *Instituto de Física da Universidade de São Paulo, Departamento de Física Nuclear, Caixa Postal 66318, São Paulo, Brazil.*

<sup>2</sup> *Universidade Federal Fluminense, Instituto de Física, Niteroi, Brazil.*

## Abstract

Recent coupled channel results for the systems  $^{18}\text{O} + ^{58,60,68}\text{Ni}$  in the bombarding energy range  $34.5 \leq E_{\text{Lab}} \leq 65$  MeV ( $V_B \approx 42.0$  MeV) are presented. In the calculations we have used the parameter free São Paulo potential as the bare interaction. The inelastic target and projectile excitations, the one ( $^{18}\text{O}$ ,  $^{17}\text{O}$ ) and the two ( $^{18}\text{O}$ ,  $^{16}\text{O}$ ) neutron transfer reactions were considered as the main channel couplings. The overall agreement with existing experimental data is quite good. Our calculations predict an unexpected fusion hindrance for above barrier energies with an important contribution of the neutron transfer channel. The sub-barrier fusion enhancement predicted by the calculations is consistent with the nuclear structure in the Ni region.

## I – Introduction

The São Paulo Potential (SPP) [1, 2, 3] microscopic bare interaction has provided a reliable starting point for the analysis of nuclear reactions by coupled channel (CC) calculations [4, 5]. It has been successfully applied in the description of elastic scattering, peripheral reaction channels and fusion for several systems with stable and exotic projectiles for bombarding energies up to 200 MeV/nucleon. The São Paulo potential is based on the Pauli non locality and was derived from the Ffran-Lemmer [6] *ansatz* for a nuclear potential with a non locality range (b):

$$V(\vec{r}, \vec{r}') = U \left( \frac{\vec{r} + \vec{r}'}{2} \right) e^{\left( \frac{\vec{r} - \vec{r}'}{b} \right)^2} \frac{1}{\pi^{3/2} b^3} \quad (1)$$

This potential has been successful applied in the description of neutron-nucleus scattering by Perey and Buck [7]. From those analyses an energy independent

---

<sup>a</sup> Dedicated to M.A. Cândido Ribeiro (1960 – 2003).

parameter ( $b_0 = 0.85$  fm) was deduced. Later on, Jackson and Johnson [8] applied this kind of analysis to  $\alpha$ -nucleus scattering in order to explain the energy dependence of optical potentials which fit the experimental data. The formalism above has been extended (*Brazilian group*) to heavy systems by deducing a general expression for the non local ( $\mathbf{b} = \mathbf{b}_0/\mu$ ) parameter. In such conditions a global expression (2) for the non local interaction has been established:

$$V(\vec{R}, \vec{R}') = V_F(R) e^{-\left(\frac{\vec{R} - \vec{R}'}{b}\right)^2} \frac{1}{\pi^{3/2} b^3} \quad (2)$$

$V_F(R)$  is the well known double folding potential. The associated parameter-free local equivalent interaction  $V_{LE}$ , that is known as the São Paulo potential [3], has the following expression:

$$V_{LE}(R, E) = V_F(R) e^{-\left(\frac{v(R)}{c}\right)^2} \quad (3)$$

where  $v(R) = \sqrt{\frac{2}{\mu}(E - V_C(R)) - V_{LE}(R, E)}$  is the relative local velocity for the colliding nuclei.

For heavy systems at the barrier radius, the effect of the Pauli non locality is quite small ( $\approx 1 - 2\%$ ). However, for a significant overlap of the target and projectile densities, this gives rise to dynamical saturation in the nuclear interaction. In our model, these effects are due to exchange of nucleons between target and projectile and they are calculated in a first order approach ( $k.b \ll 1$ ).

In this work we present new results using the CC/SSP approach for the systems  $^{18}\text{O} + ^{58,60,64}\text{Ni}$  in the energy interval  $34.5 \leq E_{\text{Lab}} \leq 65$  MeV. The  $\ell = 0$  average barrier ( $V_B$ ) value is about 42 MeV in the lab system. The inelastic target and projectile excitations, one ( $^{18}\text{O}$ ,  $^{17}\text{O}$ ) and two ( $^{18}\text{O}$ ,  $^{16}\text{O}$ ) neutron transfer reactions were considered as the main couplings. One of the main goals of the CC data analysis was to correlate the behavior of measured fusion excitation functions [9, 10] for the systems above with the nuclear structure in the Ni region.

## **II - The problem: The fusion excitation functions for the systems $^{18}\text{O} + ^{58,60,64}\text{Ni}$ and shell structure in the Ni region**

In figure 1 (top) experimental fusion data for the systems  $^{18}\text{O} + ^{58,60,64}\text{Ni}$  obtained with the technique which consists of the time of flight method combined

with an electrostatic deflector, are presented. Even considering that absolute normalization for cross sections are defined with an accuracy about 15 - 20%, the relative behavior between the systems should be reliable. In such conditions, the fusion cross sections for the system  $^{18}\text{O} + ^{58}\text{Ni}$  are enhanced with respect to those for the systems  $^{18}\text{O} + ^{60,64}\text{Ni}$ , for near and below barrier energies. If we consider that: **a)** the inelastic excitations are important couplings for the fusion channel in the barrier energy region; **b)** as shown in fig. 1 (bottom) the variation of the  $B(E2)$  values as a function of atomic mass number for the Ni isotopes presents a maximum for the  $^{60,62}\text{Ni}$  nuclei. Apparently there is a contradiction between the relative behavior of fusion excitation functions (fig. 1) and nuclear structure proprieties in the  $f$ - $p$  shell. Also, based on **Threshold Anomaly** arguments, a sharper closure of the reaction channels for decreasing energies of the  $^{18}\text{O} + ^{58}\text{Ni}$  system, particularly with respect to the  $^{18}\text{O} + ^{60}\text{Ni}$  system is expected. The  $^{58}\text{Ni}$  nucleus is the nearest even-even Ni isotope relative to the doubly magic  $^{56}\text{Ni}$  in the region (see fig. 1 bottom).

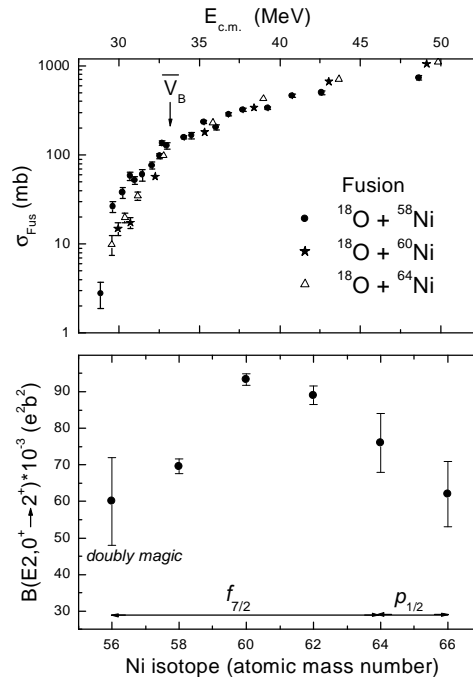


Fig – 1: (Top) - measured [9,10] fusion excitation functions for the systems  $^{18}\text{O} + ^{58,60,64}\text{Ni}$ . (Bottom) - variation of the  $B(E2)$  values as function of the Ni atomic mass number.

### III - Coupled channel calculations for the $^{18}\text{O} + ^{58,60,64}\text{Ni}$ systems

The main features of the present parameter free CC calculations are listed below:

1 -: The  $0_{\text{gs}}^+$ ,  $2_1^+$  (one phonon),  $2_2^+$ ,  $0_2^+$ ,  $4^+$  (two phonon) ( $^{58,60,64}\text{Ni}$ ) and the  $0_{\text{gs}}$ ,  $2^+$  ( $^{18}\text{O}$ ) states were considered in the calculations. The corresponding deformation parameter  $\beta_c$  and  $\beta_n$  were obtained from the literature.

2 - An  $S = 0$  form factor has been assumed for the  $2n$  transfer reactions.

3 - For the ( $^{18}\text{O}$ ,  $^{16}\text{O}$ ) reactions, excited states with energies up to 6 MeV have been considered.

4 - The corresponding average spectroscopic factors (sf) have been determined from previous near barrier  $2n$  transfer ( $^{18}\text{O}$ ,  $^{16}\text{O}$ ) reaction cross section measurements [11].

5 - For the one neutron transfer ( $^{18}\text{O}$ ,  $^{17}\text{O}$ ) reaction the corresponding sf factors have determined from previous sub-barrier energy measurements or from reported (d, p) reactions.

6 - No surface optical imaginary potential has been used in the present CC calculations.

7 - About 400 partial waves have been considered in the calculations.

8 - The  $^{18}\text{O}$  density was experimentally determined from a quasi-elastic data analysis at sub-barrier energies [11] while those for Ni isotopes were derived from Hartree-Fock-Bogoliobov calculations as reported in ref. 3.

9 - The CC calculations are quite sensitive to the bare potential; for instance, a variation of about 10% in the diffuseness parameter of the  $^{18}\text{O}$  density (Fermi-Dirac shape), sharply deteriorates the agreement with the experimental data.

10 - The present CC experimental data analyses were performed for about 60 reaction cross section measurements for the inelastic, one and two neutron transfer and the fusion processes. In the next section, some examples of the comparisons between the theoretical calculations and the experimental data are shown.

## **IV – Results**

### **IV.1 - Elastic scattering**

In figures 2 and 3, the comparisons between the CC calculations results and the existing experimental data [10,12] for elastic channel for the  $^{18}\text{O}+^{58}\text{Ni}$ ,  $^{18}\text{O}+^{60}\text{Ni}$  and  $^{18}\text{O}+^{64}\text{Ni}$  systems, respectively in the energy range  $38.1 \leq E_{\text{Lab}} \leq 63$  MeV are shown. In the figures the dash, dot, dash-dot and dash-dot-dot and solid curves correspond to CC results for no couplings (bare), only inelastic excitations (inel.), inel. plus one neutron transfer, inel. plus two neutron transfer couplings and full calculation, respectively. The agreement between the experimental data and the free parameter calculations is quite good.

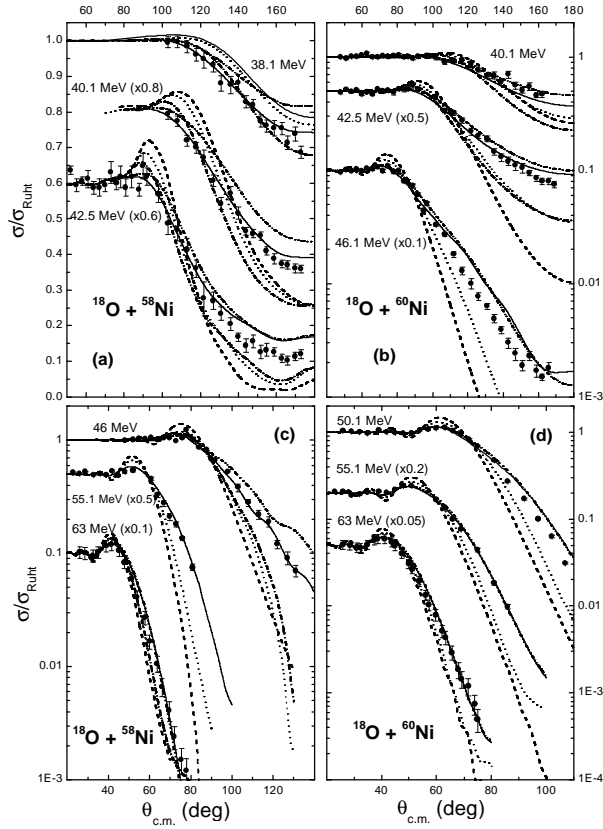


Fig. 2: CC calculation results as compared with measured [10, 12] elastic scattering angular distributions for the systems  $^{18}\text{O} + ^{58}\text{Ni}$  and  $^{18}\text{O} + ^{60}\text{Ni}$ . Lines in the figure: solid (full CC), dot (only inelastic excitations), dash-dot (inel. + 1n transfer), dash-dot-dot (inel. + 2n transfer) and dash (no couplings).

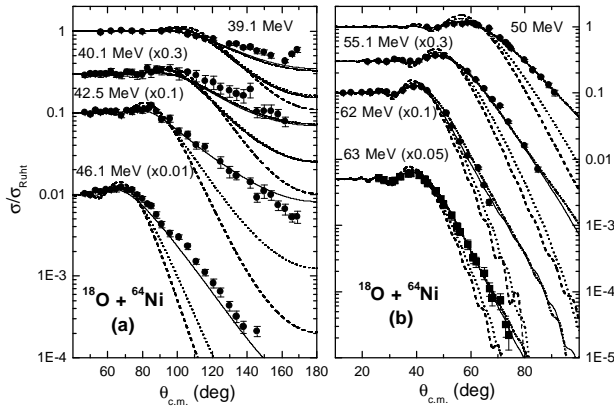


Fig. 3: The same as figure 2, for the system  $^{18}\text{O} + ^{64}\text{Ni}$ .

Considering the bare results as the reference to characterize the importance of the reaction couplings to the elastic channel:

1 - The inelastic coupling effects are quite small for the system  $^{18}\text{O} + ^{58}\text{Ni}$ , particularly as compared with those for the  $^{18}\text{O} + ^{60}\text{Ni}$  system.

2 - For  $^{18}\text{O} + ^{58}\text{Ni}$  in the barrier region, the full CC results for the inelastic scattering channel are defined by the competition between the 1 and 2 neutron transfer couplings.

3 - For the  $^{18}\text{O} + ^{60,64}\text{Ni}$  systems the effect of the one neutron couplings are quite small, because the corresponding  $Q_{gs}$  values become more negative for neutron rich

target nuclei ( $Q_{\text{optimum}}$  matching). In this situation the full CC results for the inelastic scattering channel are defined by the inelastic and two neutron transfer couplings.

4 - The importance ( $^{18}\text{O}$ ,  $^{16}\text{O}$ ) couplings is connected to the behavior of the corresponding average  $\bar{sf}$  values. Thus, for the  $^{18}\text{O} + ^{60}\text{Ni}$  ( $\bar{sf} \approx 0.2$ ) system the coupling effects are diminished relative to those of the  $^{18}\text{O} + ^{58}\text{Ni}$  ( $\bar{sf} \approx 0.8$ ) and  $^{18}\text{O} + ^{64}\text{Ni}$  ( $\bar{sf} \approx 0.6$ ) systems.

5 - For above barrier energies ( $E_{\text{Lab}} \geq 50$  MeV), the full CC results for the elastic channel are defined essentially by the bare results.

## IV.2 - Inelastic Excitations

In figures 4 and 5 the comparisons of the CC results with the experimental cross sections of the inelastic ( $2^+_1$ ) excitation for the  $^{18}\text{O} + ^{60}\text{Ni}$ , at  $E_{\text{Lab}} = 63, 34.5, 35.5, 37$  and  $38$  MeV are shown. There is good agreement between the data and the theoretical calculations. The CC result (solid lines in the figures) are defined by the inelastic excitations (dot lines) with a small contribution ( $\leq 20\%$ ) of the 2n transfer couplings, particularly for  $\theta_{\text{c.m.}} > 50^\circ$ .

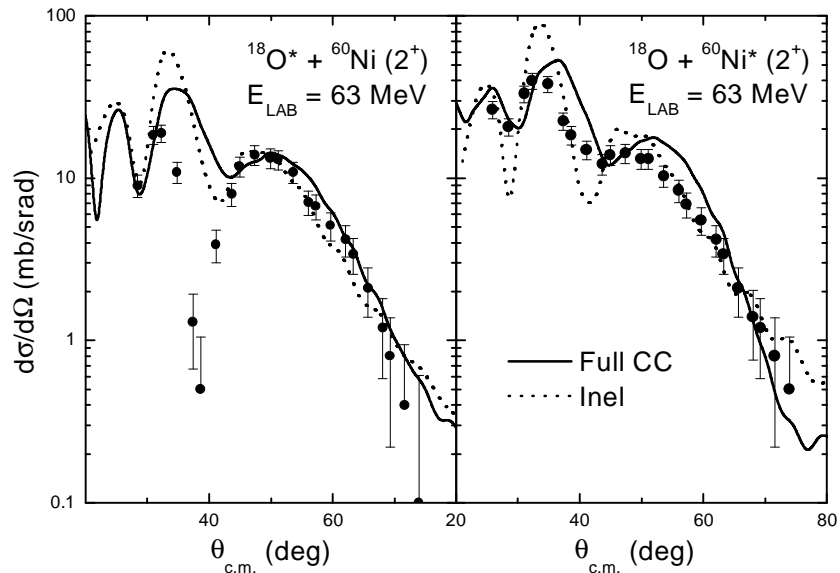


Fig. 4: CC calculation results as compared with measured [12] angular distributions of the  $2^+_1$  excited state of the  $^{18}\text{O}$  and  $^{60}\text{Ni}$  nuclei, at  $E_{\text{Lab}} = 63$  MeV.

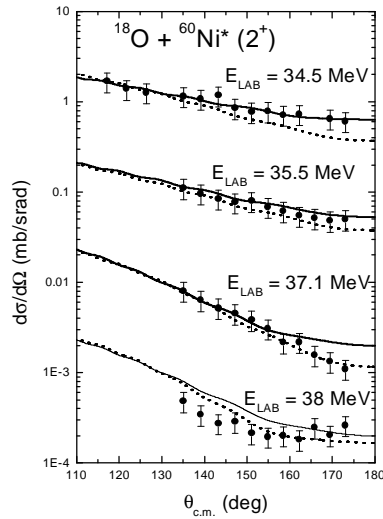


Fig. 5: The same as Fig. 4, for the  $^{60}\text{Ni}$  ( $2^+_{11}$ ) at  $E_{\text{Lab}} = 34.5, 35.5, 37.1$  and  $38$  MeV. The experimental data are from ref. 10 and 11.

### IV.3 - Transfer reactions

In figure 6, the comparisons between the experimental data and the corresponding CC results for the two neutron transfer reactions for the systems  $^{18}\text{O} + ^{58}\text{Ni}$  and  $^{18}\text{O} + ^{60}\text{Ni}$  at  $E_{\text{Lab}} = 63$  MeV are shown. We point out the good agreement between the calculations (solid lines) and the experimental data (closed circles). We observe that the oscillatory behavior presented by the measured angular distributions for the  $^{18}\text{O} + ^{60}\text{Ni}$  system (fig. 6 – left side), is correctly described by the calculations. This effect is due to the interference between incoming and outgoing waves in the 2n transfer reaction.

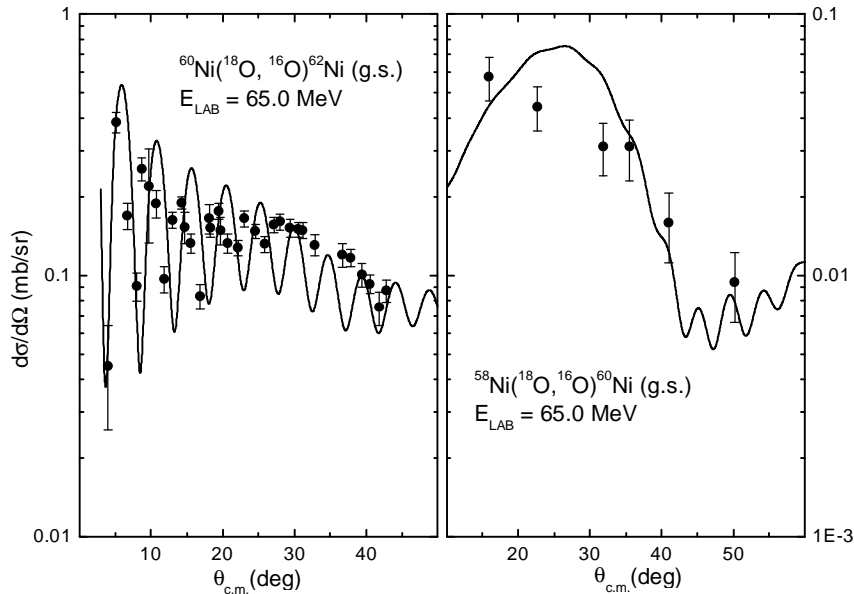


Fig. 6: CC calculation results as compared with measured [13] angular distributions for the reactions  $^{60}\text{Ni}(^{18}\text{O}, ^{16}\text{O})^{62}\text{Ni}$  (g.s.) (left side) and  $^{58}\text{Ni}(^{18}\text{O}, ^{16}\text{O})^{60}\text{Ni}$  (g.s.). The solid line corresponds to the full CC calculations.

## IV.4 - Fusion

In figure 7 the corresponding CC results for the fusion for the systems  $^{18}\text{O} + ^{58,60,64}\text{Ni}$  are shown. The agreement between the theoretical predictions and the experimental data is good. Based on the bare results, the sub barrier enhancement for the three systems are compatible with the nuclear structure in the Ni region. We point out the sharper closure of the fusion channel for decreasing energies for the system  $^{18}\text{O} + ^{58}\text{Ni}$ , particularly in relation to that for  $^{18}\text{O} + ^{60}\text{Ni}$ . We note also a pronounced fusion hindrance for slightly above barrier energies, particularly for  $^{18}\text{O} + ^{58}\text{Ni}$ . This effect, mainly attributed to the 2n transfer coupling channel, is strongly diminished for  $^{18}\text{O} + ^{60}\text{Ni}$ , and is somewhat important for the  $^{18}\text{O} + ^{64}\text{Ni}$ . The behavior above is accompanied by the corresponding average  $\bar{sf}$  values for the transfer reactions  $^{58}\text{Ni}(^{18}\text{O}, ^{16}\text{O})^{60}\text{Ni}$  ( $\bar{sf} \approx 0.8$ ),  $^{60}\text{Ni}(^{18}\text{O}, ^{16}\text{O})^{62}\text{Ni}$  ( $\bar{sf} \approx 0.2$ ) and  $^{64}\text{Ni}(^{18}\text{O}, ^{16}\text{O})^{66}\text{Ni}$  ( $\bar{sf} \approx 0.6$ ), respectively. The one neutron transfer coupling is only important for the  $^{18}\text{O} + ^{58}\text{Ni}$  system due to  $Q_{\text{optimum}}$  matching, as discussed above for the elastic channel. Thus, based on the CC theoretical predictions for  $^{18}\text{O} + ^{58,60,64}\text{Ni}$  systems, it was possible to describe the corresponding fusion data coherently with the nuclear structure in the Ni region.

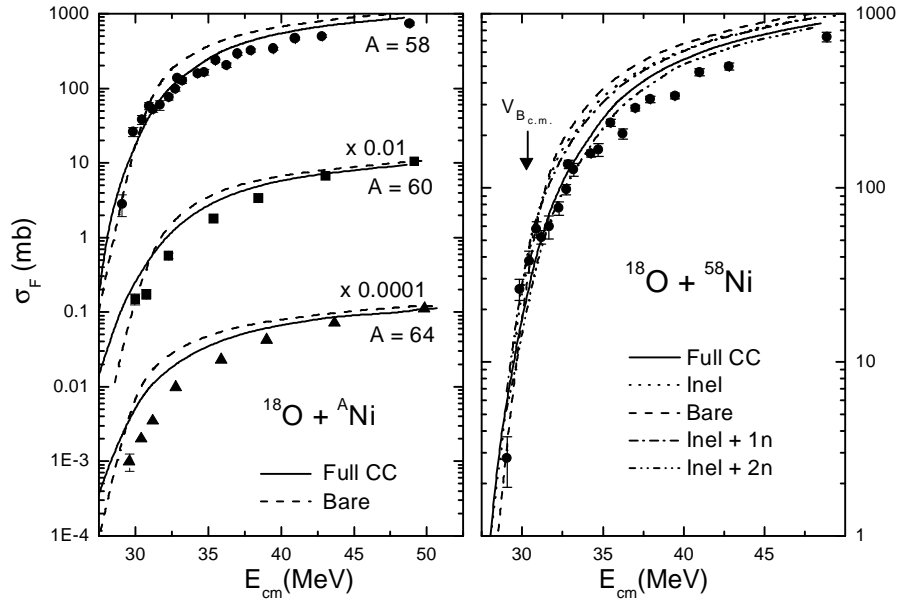


Fig. 7: (Left side) – fusion excitation functions for the systems  $^{18}\text{O} + ^{58,60,64}\text{Ni}$  as compared with full CC (solid lines) and no couplings (dashed lines) results. (Right side) – fusion excitation function for the systems  $^{18}\text{O} + ^{58,60,64}\text{Ni}$  as compared with full CC prediction (solid line), only inelastic excitations (dot line), no couplings (dashed line), inel. + 1n transfer (dash-dot line) and inel. + 2n transfer (dash-dot-dot line).



## V - Conclusions

In this work we have presented consistent parameter free coupled channel calculations, which describe the near barrier energy experimental data for the systems  $^{18}\text{O} + ^{58,60,64}\text{Ni}$ . The exciting experimental cross sections of about sixty reactions of the elastic, inelastic excitations and one and two neutron transfer processes have been analyzed. The agreement between the calculations and the data is quite good. Our theoretical data analysis also predicts the coexistence of fusion enhancement and hindrance consistent with the nuclear structure in the Ni region and *threshold anomaly* arguments.

## VI - References

- 1 - M.A.Cândido Ribeiro, L.C. Chamon, D. Pereira, M.S. Hussein, D. Galleti, Phys. Rev. Lett. 78 (1997) 3270.
- 2 - L.C. Chamon, D. Pereira, M.S. Hussein, M.A. Cândido Ribeiro, D. Galleti, Phys. Rev. Lett. 79 (1997) 5218.
- 3 - L.C. Chamon, B.V. Carlson, L.R. Gasques, D. Pereira, C. De Conti, M.A.G. Alvarez, M.S. Hussein, M.A. Cândido Ribeiro, E.S. Rossi Jr., C.P. Silva, Phys. Rev. C66 (2002) 014610.
- 4 - J.J.S. Alves, P.R.S. Gomes, J. Lubian, L.C. Chamon, D. Pereira, R.M. Anjos, E.S. Rossi Jr., C.P. Silva, M.A.G. Alvarez, G.P.A. Nobre, L.R. Gasques, Nucl. Phys. A748 (2005) 59.
- 5 - D. Pereira, C.P. Silva, J. Lubian, E.S. Rossi Jr., L.C. Chamon, Phys. Rev. C73 (2006) 014601.
- 6 - W.E. Ffran and R.H. Lemmer, Nuovo Cimento 5 (1957) 1654.
- 7 - F. Perey and B. Buck, Nucl. Phys. 32 (1962) 253.
- 8 - D.F. Jackson and R.C. Johnson, Phys. Lett. 49B (1974) 249.
- 9 - A.M. Borges, C.P. Silva, D. Pereira, L.C. Chamon, E.S. Rossi Jr., C.E. Aguiar, Phys. Rev. C46 (1992) 2360.

10 - C.P. Silva, D. Pereira, L.C. Chamon, E.S. Rossi Jr., G. Ramirez, A.M. Borges, C.E. Aguiar, Phys. Rev. C55 (1997) 3155.

11 - E.S. Rossi Jr., D. Pereira, L.C. Chamon, C.P. Silva, M.A.G. Alvarez, L.R. Gasques, J. Lubian, B.V. Carlson, C. De Conti, Nucl. Phys. A707 (2002) 325.

12 - K.E. Rehm, H. J. Körner, M. Richter, H. P. Rother, J. P. Schiffer, and H. Spieler, Phys. Rev C12 (1975) 1945.

13 - E.H. Auerbach, *et al.*, Phys. Rev. Lett. 30 (1973) 1078.